

PACS numbers: 42.15.Eq, 42.25.Fx, 42.25.Hz, 42.25.Ja, 42.25.Lc, 42.62.Be
DOI: 10.1070/QE2008v038n07ABEH013857

Fibreoptic methods of cross-polarisation optical coherence tomography for endoscopic studies

V.M. Gelikonov, G.V. Gelikonov

***Abstract*. Two systems of cross-polarisation optical coherence tomography based on polarisation-maintaining and polarisation non-maintaining fibres intended for *in vivo* endoscopic studies of biological objects are described. The sensitivities of the systems detecting scattered light with the initial and orthogonal polarisations in media with local microscopic optical anisotropic inhomogeneities are compared.**

Keywords: *cross-polarisation optical coherence tomography, single-mode optical fibre, orthogonally polarised modes.*

1. Introduction

Optical coherence tomography (OCT) is a noninvasive method for studying the internal structure of the surface layers of biological tissues in the near-IR range with a spatial resolution of 1 – 15 μm [1]. The OCT study of the structure of mucous and serous tissues of inner human organs became possible after the development of flexible endoscopic miniature probes with transverse electromechanical scanning [2]. One of the directions of OCT studies providing additional information on the structure and state of biological tissues is based on the use of polarisation methods [3 – 25] which can increase the information content and specificity of *in vivo* endoscopic OCT diagnostics.

Light backscattered from a biological tissue can exhibit regular and irregular variations in the polarisation state. Thus, the average velocity of an optical wave in some tissues containing regular structures depends on the electric vector direction (optical birefringence) [26]. This leads to a change in the polarisation state of backscattered waves. Because scattered radiation is detected locally by the OCT method, optical birefringence can be determined as a function of the observation depth. This principle is used in polarisation-sensitive OCT (PS OCT) which allows the imaging of optical birefringence in ordered biological tissues [3 – 5, 7, 10, 16, 17] and measuring the Stokes parameters of scattered light [9, 11, 15] as functions of the depth. The value of birefringence in a biological tissue can be used, in particular, as an optical marker to estimate the state of burnt tissues [4, 5, 7], for the earlier glaucoma diagnostics [21], etc.

Birefringence is weak in most tissues and cannot be detected by the OCT method. Light scattered from randomly oriented inhomogeneities can have orthogonal polarisation [6, 8]. The degree of such scattering depends on the structure, anisotropy, and size of optical inhomogeneities and is determined by the tissue type and state. The differences and features of scattering of light into orthogonal polarisation in the case of inflammatory processes and in cicatrical and cancer tissues of esophagus observed in [27, 28] were related by the authors to the state of collagen. The usual OCT images of these tissues are structureless. Imaging and a comparison of the images of the transverse scattering pattern in biological tissues in the initial and orthogonal polarisations are used in another, less studied OCT method, which can be called cross-polarisation OCT (CP OCT) [6, 8, 13, 27 – 29].

PS OCT methods impose strict requirements on the optical scheme to provide a weak enough optical coupling between both channels detecting light with orthogonal polarisations. This concerns to the greatest extent the CP OCT method in which the informative cross-polarisation scattering signal is observed in a large dynamic range against the noise background [6, 8]. The basic optical scheme [6] contains a free space mirror interferometer with discrete elements. The polarisation state of light in each of the arms of the interferometer can be precisely controlled. Optical fibres, which are used in OCT methods to allow bendings of the signal arm and compactness of the optical scheme, produce phase distortions; nevertheless, they are employed in a number of polarisation-sensitive methods. Thus, a single-mode (SM) fibre is applied to filter spatially incoherent light emitted from the signal and reference arms in the directional detector scheme [5, 6].

Setups for polarisation-sensitive OCT of the next generation use interferometers based on isotropic SM fibres [11, 16, 17]. The influence of random birefringence in these interferometers caused by the ellipticity of the SM fibre core and noncircular stress distribution was reduced either by compensating the intrinsic and induced birefringence or modulating the polarisation state [11]. Conventional OCT interferometers based on polarisation-maintaining (PM) fibres cannot be used in polarisation-sensitive OCT described above due to a large difference in phase incursions in orthogonal waves at which these waves become incoherent. However, OCT interferometers using such PM fibres can be applied in the CP OCT method, which does not require the removal of the polarisation-mode dispersion [8].

V.M. Gelikonov, G.V. Gelikonov Institute of Applied Physics, Russian Academy of Sciences, ul. Ul'yanova 46, 603950 Nizhnii Novgorod, Russia; e-mail: gelikon@ufp.appl.sci-nnov.ru, grig@ufp.appl-sci-nnov.ru

Received 1 April 2008; revision received 30 May 2008
Kvantovaya Elektronika **38** (7) 634 – 640 (2008)
Translated by M.N. Sapozhnikov

A disadvantage of polarisation-sensitive schemes using PM fibres is the complication of the cross-correlation function of the interferometer caused by parasitic coupling between normal modes.

In this paper, we present the results of the development of efficient schemes for CP OCT with the successive detection based on PM fibres. These schemes can be also used for birefringent measurements.

2. Two-polarisation CP OCT based on PM fibres with the separate detection and a linearly polarised probe wave

A PM fibre was first used in a single-detector scheme of the temporal OCT method to eliminate the influence of bendings of a signal arm on measurements and to develop new methods of transverse scanning [30]. This allowed the development of the endoscopic applications of the method [2]. In the first fibre realisation of the CP OCT method, when an object was probed by linearly polarised light and signals with the initial and orthogonal polarisations were detected successively, only motionless samples were studied [8]. In this case, light polarised orthogonally to the probe-beam polarisation was detected by placing a 45° Faraday cell into the reference arm of a Michelson interferometer [8, 28]. In the case of moving (living) objects, scattered light with initial and orthogonal polarisations should be detected simultaneously. Such a two-channel correlation detection based on the difference in the velocities of natural polarisation waves in the PM fibre can be used both in PS OCT and CP OCT.

Figure 1 presents the scheme of the experimental setup based on a fibreoptic Michelson interferometer used in these methods. The 950-nm IR radiation ($\Delta\lambda = 60$ nm) from a superluminescent diode (SLD) passed through an optical isolator and an isotropic fibre. The linear component of radiation was oriented along the maximum transmission axis of a polariser with the help of the first Lefebvre polarisation controller (PC1) [31]. By using a PC2, linearly polarised radiation was oriented at the interferometer input along one of the anisotropic axes of the PM fibre. A quarter-wave phase plate oriented at 22.5° to the axis of one of the natural waves was placed into the reference arm. As a result, an additional orthogonal component of light with intensity equal to that of the reference wave with the initial polarisation was produced during the backward propagation of the wave.

In the first channel, light was detected which passed through the signal and reference arms of the interferometer in both directions with the initial linear x-polarisation. In the second (orthogonal) channel, light passing forward in both interferometer arms also had x-polarisation. The polarisation state of light propagating backward in both arms was changed to orthogonal (y). As a result, the total optical path of the light differed from that in the first channel. The optical path difference $\Delta L_p = L_f \Delta n_f = 2.4$ mm of orthogonally polarised waves in each of the interferometer arms (of lengths $L_f = 12$ m) greatly exceeded the coherence length $L_c = 12$ μm (here, $\Delta n_f = 2 \times 10^{-4}$ is the difference for the slow and fast waves in the PM fibre). This provided the efficient optical isolation between the channels, which is necessary for CP OCT studies. In this case, the waves of each of the orthogonal interfered independently but at the same optical path difference in the interferometer arms. Note that the length of the interferometer arms was mainly determined by the length of the fibre used in piezo-fibre delay lines [32]. Then the waves with orthogonal polarisations were separately directed by a polarisation beamsplitter to two photodetectors and were simultaneously subjected to analogue and digital processing in two independent identical channels. The two-dimensional images of the scattering pattern in both polarisations were visualised on the computer display, both separately and with a mutual superposition in additional colours. The precise superposition of the image elements was provided by the simultaneous detection of signals.

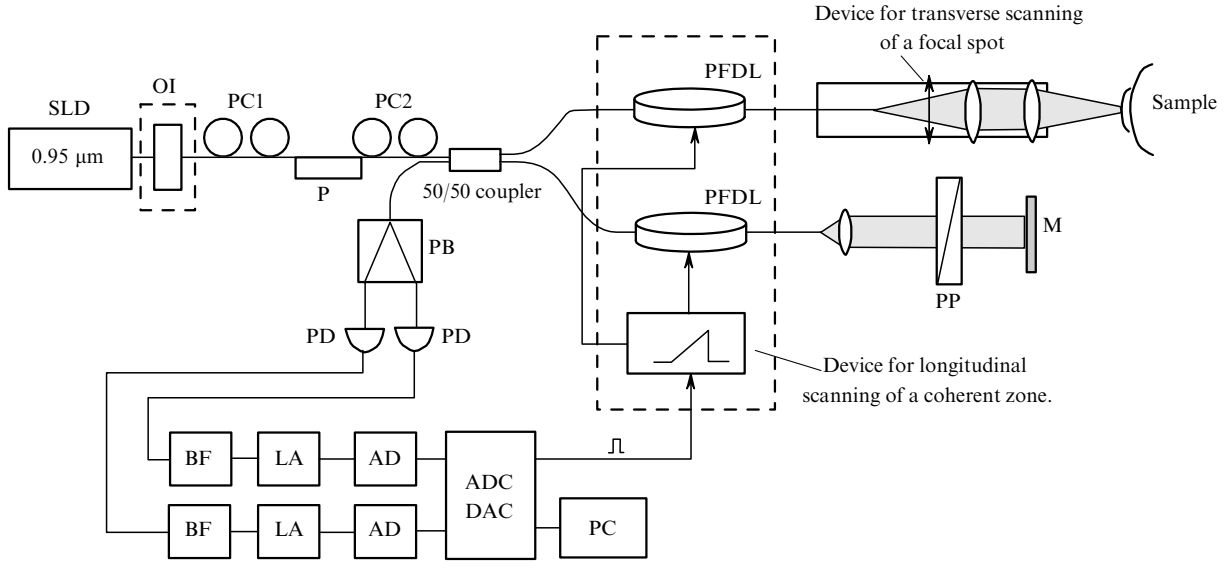

Figure 1. Experimental setup for CP OCT: (SLD) superluminescent diode; (OI) optical isolator; (PC1, PC2) polarisation controllers; (PFDL) piezofibre delay line; (PP) phase plate (Faraday cell); (M) mirror; (P) polariser; (PB) polarisation beamsplitter; (PD) photodiode; (BF) band filter; (LA) logarithmic amplifier; (AD) amplitude detector; (PC) personal computer; (ADC) analogue-to-digital converter; (DAC) digital-to-analogue converter.

The maximum information content of the CP OCT method is achieved at the maximum dynamic range of a signal in the orthogonal channel upon detecting signal at the dark level. For this purpose, the influence of parasitic coherent waves caused by the imperfection of the optical path was reduced to minimum. In addition, the influence of the incoherent response of backscattered interfering waves to the SLD was efficiently eliminated due to optical isolation. As a result, the dynamic range of signals in the orthogonal channel achieved 35–40 dB, which allowed the detection of light at the noise level. An advantage of this scheme is a constant linear polarisation of the probe wave, which allowed us to determine the orientation of the anisotropy axis of the biological object. Figure 2 demonstrates the CP OCT images of skin (without averaging over A and B scans) in the initial linear and orthogonal polarisations, which were obtained with the help of an endoscopic probe pressed to a finger.

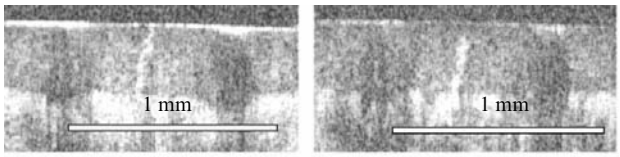

Figure 2. CP OCT images of a finger skin in the initially (a) and orthogonally (b) polarised light.

3. Cross-polarisation OCT with a SM fibre

An important aspect in the development of endoscopic applications of the OCT method is the interchangeability of endoscopic probes, which is difficult to provide in the above-described scheme because of a large length of interferometer arms and the insufficient stability of parameters of a PM fibre. The interchangeability can be provided by using an optical scheme with an isotropic fibre, in which a measuring Fizeau interferometer is added to a Michelson interferometer that is used only as a correlator [33]. The Fizeau interferometer sums up the waves reflected from the end of an isotropic fibre probe and an object under study with the optical path difference of about 2 cm. Because this difference is mainly formed in the air gap of the Fizeau interferometer and in a lens system, the probes can be easily reproduced.

A special problem in the OCT method with a SM fibre is the performance of polarisation measurements. Indeed, because of the possible movements of the probe during measurements, the polarisation of the initial probe wave is arbitrary, elliptical, and changes with time. Therefore, it is necessary not only to produce an adaptive orthogonal reference wave, but also to perform the separate and independent detection of interference signals in both orthogonal polarisations.

The CP OCT method with an isotropic fibre is based on the two key ideas [34]. First, as follows from the equivalence theorems of polarisation optics and optics of single-mode fibres [35], in the case of coherent radiation an isotropic single-mode fibre at any phase perturbations is characterised by two normal linear orthogonally polarised waves. It is easy to show that for any phase perturbations and in the absence of anisotropic losses, the two waves (not only normal) preserve their orthogonality during propagation in a SM fibre despite a change in the polarisation state. Indeed, for any phase perturbations and in the absence of anisotropy of losses, the Jones matrix $\hat{A}$ of such an optical system is unitary. If the elliptically polarised wave $\boldsymbol{E}_u$ with an arbitrarily oriented principal axis of the ellipse and the orthogonal wave $\boldsymbol{E}_v$, for which the orthogonality condition $(\boldsymbol{E}_u, \boldsymbol{E}_v = 0)$ is fulfilled, are coupled to a fibre described by the matrix $\hat{A}$, the orthogonality condition $(\boldsymbol{E}_u^{\text{out}}, \boldsymbol{E}_v^{\text{out}}) = (\hat{A}\boldsymbol{E}_u, \hat{A}\boldsymbol{E}_v) = (\boldsymbol{E}_u, \boldsymbol{E}_v) = 0$ will be also fulfilled for output waves with vectors $\boldsymbol{E}_u^{\text{out}} = \hat{A}\boldsymbol{E}_u$ and $\boldsymbol{E}_v^{\text{out}} = \hat{A}\boldsymbol{E}_v$ because the scalar product of two vectors is preserved after multiplication by a unitary operator [36].

Note that if the path difference of the orthogonal modes does not exceed the coherence length, this is also valid for low-coherence radiation. In the CP OCT method considered here, the orthogonality of waves in an isotropic fibre, of course, should be preserved not only for regular waves but also for backscattered waves.

The second idea is the generation of two strictly orthogonally polarised waves with a certain delay between coherent trains at the optical scheme input. In the general case these waves can have arbitrary ellipticity under the condition of their mutual orthogonality. By using the optical scheme of a Fizeau interferometer in a probe, each of the two waves can be divided into the reference and probe waves without changing their polarisation state. Both these ideas were used to realise the CP OCT method based on the fibreoptic scheme presented in Fig. 3. The prototype of the optical scheme is described in [37].

The optical scheme, containing a measuring Fizeau interferometer, a common optical part for signal and reference waves [38] and a autocorrelator based on a Michelson interferometer with Faraday mirrors [39, 40], is made by using a SMF-28 isotropic SM fibre. Both waves ($\lambda = 1300$ nm, $\Delta\lambda = 35$ nm) in the Fizeau interferometer reflected from the fibre end produce a system of two orthogonal reference waves with the specified delay, which allows the heterodyne detection of weak scattered light with the same polarisation state and a stable visibility of the interference pattern. To our knowledge a fibreoptic Fizeau interferometer was first applied for measuring subangström vibrations [38]. An autocorrelator based on a Michelson interferometer with Faraday mirrors is isotropic and efficient for any input polarisation state. Note that the method of compensation of arbitrary anisotropy in single-mode fibres by using a Faraday mirror was first proposed and demonstrated in our papers [41, 42]. This method was also proposed later in [43–47].

The scheme operates as follows. Partially polarised SLD radiation is delivered through a SM fibre to a PC1. The latter is used to excite two mutually coherent orthogonal linearly polarised waves $\boldsymbol{x}_0 E_x$ and $\boldsymbol{y}_0 E_y$ with the same intensities at the input of a polarisation mode delay former (DF) made of a birefringent fibre. These waves are the natural normal waves of a PM fibre (notation in the moving coordinate system). The orthogonal waves propagate over optical paths of different length in the DF, the train of the fast wave $\boldsymbol{x}_0 E_x$ overtaking the train of the slow wave $\boldsymbol{y}_0 E_y$ by a fixed base interval ΔL, which slightly exceeds (by 10 %–20 %) the A scan depth ($\Delta L = 2$ mm in our setup). The large intrinsic birefringence of this PM fibre provides the

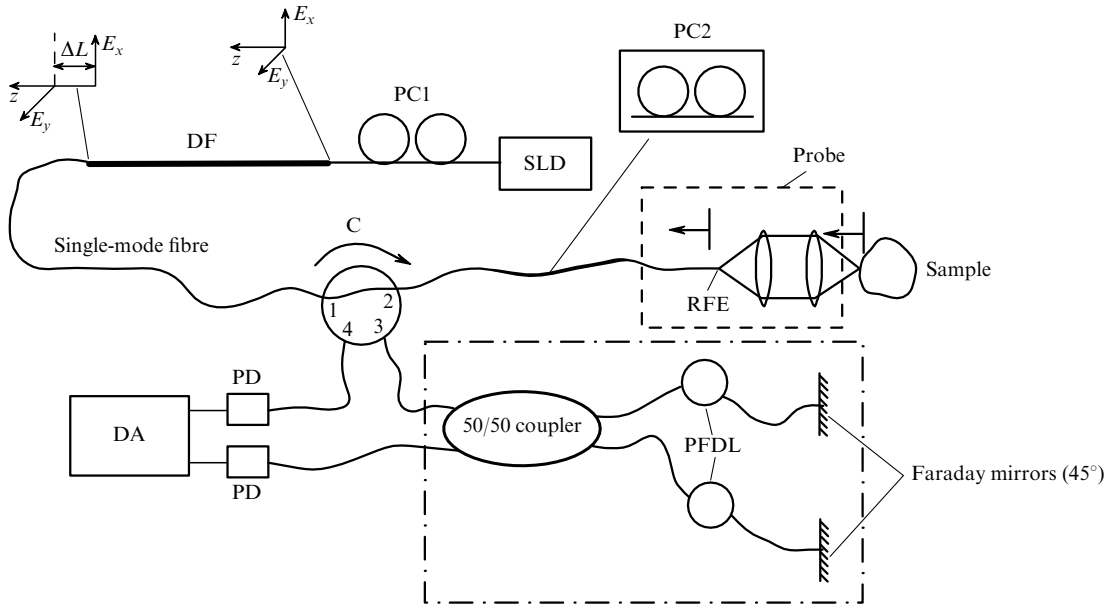

Figure 3. Optical scheme of the CP OCT setup: (SLD) superluminescent diode; (PC1, PC2) polarisation controllers; (DF) polarisation mode delay former consisting of a birefringent fibre; (C) four-port circulator; (RFE) reflecting fibre end; (PFDL) piezofibre delay line; (PD) photodiode; (DA) differential amplifier. The dashed frame singles out the probe and the dot-and-dash frame singles out the compensating Michelson interferometer which also performs the longitudinal A scan.

absence of parasitic coherent waves at the input of the DF from which light is coupled to the main optical scheme based on a SM fibre and excites at its input the orthogonally polarised waves $\boldsymbol{x}_0 E_x$ and $\boldsymbol{y}_0 E_y$ with the same optical path difference. During the propagation of the waves $\boldsymbol{E}_u$ and $\boldsymbol{E}_v$ in the optical scheme, their polarisation becomes elliptical in the general case with changing the tilt of major axes. However, despite various perturbations of the fibre and its bendings, the orthogonality of the waves is preserved.

Consider the structure of reflected waves in a Fizeau interferometer of length ΔL_F formed by the probe fibre end and an object. To simplify the description, we introduce the Cartesian coordinate system (x, y) at the probe output, which is oriented along major axes of the polarisation ellipses of output orthogonally polarised waves. For simplicity we replace the orthogonal elliptic waves at the probe output by the orthogonal linear waves with electric vectors oriented along the major axes of polarisation ellipses (see an example in the frame in the left part in Fig. 4). We denote conventionally the states of these orthogonally polarised waves by $\boldsymbol{x}E_x$ and $\boldsymbol{y}E_y$.

Then, light is coupled through ports 1 and 2 of a circulator into the single-mode fibre of a probe shown by the dashed rectangle in Fig. 3. The reflecting end of the fibre is slightly tilted to obtain a certain fraction of reflected light (proportional to the reflectance r^2). The two reference waves $\boldsymbol{x}rE_x$ and $\boldsymbol{y}rE_y$ formed after reflection have the same optical path difference ΔL (Fig. 4). By selecting the value of r (one of the measures), the excess noise was preliminarily reduced [48]. A greater part of light is focused on a sample by a lens system. In the general case a fraction of backscattered radiation contains four waves (we will consider them in the laboratory coordinate system). Thus, the backscattering of the wave $\boldsymbol{x}E_x$ produces waves $\boldsymbol{x}K_{xx}E_x$ and $\boldsymbol{y}K_{xy}E_x$ with the initial and orthogonal polarisations, while the backscattering of the wave $\boldsymbol{y}E_y$ produces the wave $\boldsymbol{y}K_{yy}E_y$ with the same polarisation and the wave $\boldsymbol{x}K_{yx}E_y$ with the orthogonal polarisation. Scattering coefficients for radiation with the initial and orthogonal polarisations in a random medium are $K_{xx} = K_{yy}$ and $K_{xy} = K_{yx}$. Both groups of the scattered waves coupled to the fibre have the same basic delay ΔL with respect to each other as the delay between reference waves. The relative delay of the onset of the group of reference waves with respect to the group of scattered waves is equal to the doubled length ($2\Delta L_\mathrm{F}$) of the Fizeau interferometer. Both radiation portions pass through ports 2 and 3 of the circulator and enter a Michelson interferometer formed by a 50/50 coupler and single-mode fibre arms with Faraday mirrors at their ends. The scheme of relative delays for reference waves and waves scattered by the sample in the backward path before coupling into the Michelson interferometer is shown in Fig. 4.

To compensate for the initial delay, the Michelson interferometer is adjusted with the initial optical path difference in arms $2\Delta L_\mathrm{F} - \Delta L$. By changing this difference, the mutual coherence of trains is reconstructed successively and at a constant velocity with the corresponding Doppler shift of their optical spectra. The optical path difference in the Michelson interferometer arms is modulated by means

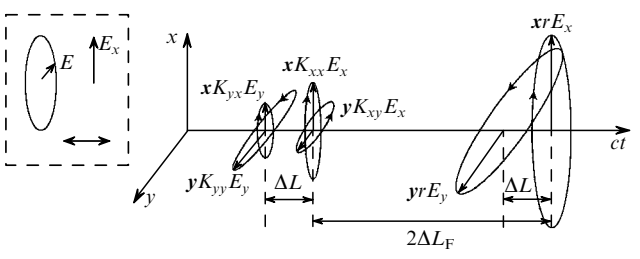

Figure 4. Path differences for reference and scattered waves.

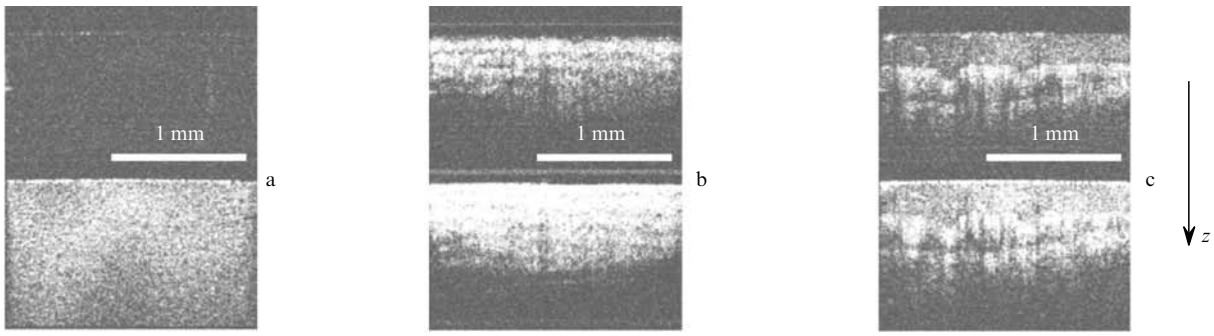

Figure 5. CP OCT images of a vacuum lubricant (a), chicken tendon (b), and human finger skin (c).

of piezofibre delay lines [32]. The sum waves from one output of the interferometer are incident on the first photodiode, and from the second one – through ports 3 and 4 of the circulator to the second photodiode. Signals at the Doppler shift frequency are then subtracted in a differential amplifier, which, as known, leads to the doubling of out-of-phase interference signals and to the subtraction of the in-phase components of disturbances and noise.

Consider the mechanism of formation of signals with orthogonal polarisations upon successive A-scans performed inside an object with the help of a Michelson interferometer. In fact this is the method for separating channels for detecting light scattered into waves with the initial and orthogonal polarisations. As show above, two groups of reference and scattered waves with the mutual spatial shift $2\Delta L_F$ propagating in a single-mode fibre arrive to the Michelson interferometer by preserving coherence and orthogonality but having an arbitrary polarisation state. Due to the use of the isotropic 50/50 coupler in the Michelson interferometer, the waves in the initial parts of fibres in the interferometer arms have the same polarisation states. It is known that, when 45° Faraday mirrors are used in the Michelson interferometer, the polarisation state of waves at its output differs from that at its input only by the rotation by 90° [41, 42]. As a result, the mutual orthogonality state is preserved in the corresponding groups of scattered and reference waves.

The compensation of the path difference between coherent components with initial and orthogonal polarisations is provided by controlling the difference of the interferometer arms. As follows from Fig. 4, for the delay $2\Delta L_F - \Delta L$, the reference wave $\boldsymbol{y}rE_y$ with the initial polarisation will interfere with the field of the wave $\boldsymbol{y}K_{xy}E_x$ scattered into the orthogonal polarisation (orthogonal channel). For the delay $2\Delta L_F$, the reference and scattered waves with initial polarisations will interfere in pairs: $\boldsymbol{x}rE_x$ and $\boldsymbol{x}K_{xx}E_x$ and also $\boldsymbol{y}rE_y$ and $\boldsymbol{y}K_{yy}E_y$ (parallel channel). The interference between the reference wave $\boldsymbol{x}rE_x$ and scattered wave $\boldsymbol{x}K_{yx}E_y$ will be observed for the delay $2\Delta L_F + \Delta L$ (second orthogonal channel). Scattering coefficients should be estimated taking into account that in the case of the delay $2\Delta L_F$, two pairs of the waves interfere, while for delays $2\Delta L_F - \Delta L$ and $2\Delta L_F + \Delta L$, only one pair of the waves interfere. It is also necessary to take into account the presence of a small incoherent component in the reference wave of orthogonal channels, which is caused by the incomplete polarisation of the light source. It is obvious that if the longitudinal scan depth overlaps not only one but two or three delays indicated above, two or three interference patterns will be successively represented during one increased A scan.

Figure 5 presents, from top to bottom along the scan direction (z), the CP OCT images of a vacuum lubricant, chicken tendon, and human finger skin. The upper image corresponds to the interference of waves $\boldsymbol{y}rE_y$ and $\boldsymbol{y}K_{xy}E_x$, the lower image corresponds to the sum of interferences of pairs of waves $\boldsymbol{x}rE_x$ and $\boldsymbol{x}K_{xx}E_x$ and also $\boldsymbol{y}rE_y$ and $\boldsymbol{y}K_{yy}E_y$. As follows from Fig. 5a, the signal of scattering to the orthogonal polarisation in a weakly depolarising model medium (vacuum lubricant) is virtually absent. According to the estimate, this signal is determined by the residual noise level, which corresponds to the large dynamic range for detecting in the orthogonal polarisation (at a level of 40 dB). The chicken tendon image (Fig. 5b) demonstrates the typical modulation of brightness caused by a strong birefringence of the medium. The images of a biological tissue – the finger skin in the orthogonal and initial polarisations (Fig. 5c) have a better quality, which is typical for the CP OCT method.

4. Estimates of the sensitivity of orthogonal detection channels in CP OCT methods with PM and isotropic fibres

The CP OCT setup using a PM fibre has the same sensitivity in both polarisation channels in the case of the efficient optical isolation of the radiation source from the optical scheme. Figure 6 presents that upon irradiation of a model sample – a sheet of dense paper impregnated with an immersion liquid, the difference of the logarithms of interference signals in both channels is virtually zero [curve (*1*)]. The paper was probed through a polarising plate turned through 45° to the linearly polarised probe wave. A small difference from zero observed in Fig. 6 can be caused by the inaccuracy in the equalisation of the sensitivity of detecting channels or by specific features of microscopic inhomogeneities in the probed region. Signals received in different channels upon probing the same sample without a polariser differ on average by ~ 4 dB [curve (*2*)]. A simple estimate shows that such inequality of signals of scattering to the initial linear and orthogonal polarisations should take place in the case of the uniform angular and spatial distribution of microscopic inhomogeneities scattering light as linear dipoles. Indeed the coefficients of scattering to the initial linear polarisation

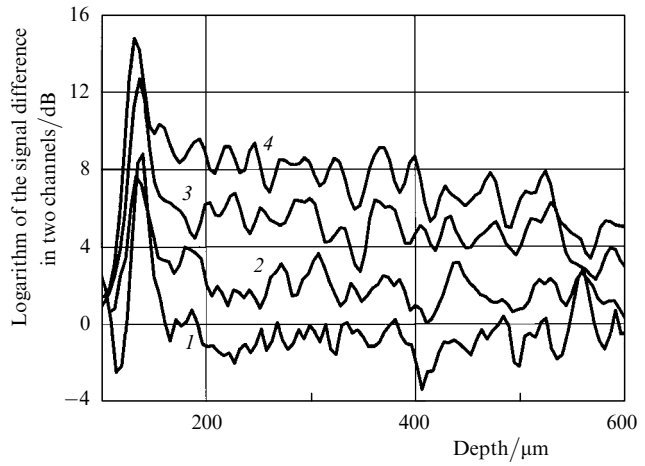

Figure 6. Difference of signals from an immersion liquid-impregnated sheet of paper in two orthogonal detection channels in a scheme based on an anisotropic fibre with an additional polariser mounted at 45° to the electric vector of the probe weave (*1*) and without the polariser (*2*), and also in a scheme based on a single-mode fibre using only one reference wave for circular (*3*) and linear (*4*) polarisations of the probe wave.

(K_{xx}) and to the orthogonal polarisation (K_{xy}) are related by the expression

$$\frac{K_{xx}}{K_{xy}} = \frac{\int_0^{\pi/2} \cos^2\psi \mathrm{d}\psi}{\int_0^{\pi/2} \cos\psi \sin\psi \mathrm{d}\psi} = \frac{\pi}{2},$$

where ψ is the angle between the unit vector $\boldsymbol{x}$ of the probe wave and a randomly oriented dipole. Because the interference signal on the photodetector load is proportional to the field, the difference of the detected signals at the logarithmic unit output is

$$U_{xx} - U_{xy} = 20\log(K_{xx}/K_{xy}) \approx 3.9 \text{ dB},$$

which coincides with the experimental result.

Thus, when the probe wave is linearly polarised, signals in the orthogonal channel are always smaller at least by 3.9 dB. The sensitivities of orthogonal channels can be equal ($U_{xx} - U_{xy} = 0$) only if the probe wave has a circular polarisation.

The same sensitivity of both polarisation channels in the PC OCT scheme with a single-mode fibre can be obtained when two conditions are fulfilled: (i) the probe wave should have circular polarisation and (ii) the interference signal between the reference ($\boldsymbol{y}rE_y$) and scattered ($\boldsymbol{y}K_{xy}E_x$) waves is added with the interference signal between the reference ($\boldsymbol{x}rE_x$) and scattered ($\boldsymbol{x}K_{yx}E_y$) waves. If these two conditions are fulfilled, $U_{xx} - U_{xy} = 0$. The relation between sensitivities in orthogonal channels was experimentally verified by controlling the polarisation state of the probe wave by means of the second polarisation controller (PC2). Curve (*3*) in Fig. 6 is a signal in the case of the circularly polarised probe wave and detecting only half the light scattered to the orthogonal polarisation, i.e. upon interference of only the reference wave $\boldsymbol{y}rE_y$ with the scattered wave $\boldsymbol{y}K_{xy}E_x$. The corresponding difference of signals in two channels is 6 dB. Curve (*4*) in Fig. 6 was obtained in the case when the probe wave was linearly polarised with the help of the PC2 and the difference of signals in the two channels was greater by another 4 dB. In the case of the elliptically polarised probe wave, the difference of signals will be between curves (*3*) and (*4*).

Thus, the maximum detection sensitivity of a wave scattered to the orthogonal polarisation can be obtained in the optical scheme with a single-mode fibre (Fig. 6) when the probe wave is circularly polarised and the waves $\boldsymbol{y}K_{xy}E_x$ and $\boldsymbol{x}K_{yx}E_y$ are simultaneously detected.

5. Conclusions

We have considered two fibreoptic schemes of the temporal CP OCT method in which an endoscopic probe can be bent during measurements. It has been shown that the optical scheme based on an isotropic fibre is most promising because it allows one not only easily to interchange endoscopic probes but also has the maximum and the same sensitivity for detecting scattered light with the initial and orthogonal polarisations. Experiments have demonstrated a high reliability of the method, a high imaging quality for both polarisations and the absence of any noticeable artefacts. The method provides high-quality images simultaneously in both polarisations in the dynamic range restricted only by the residual noise level and allows one to use a flexible isotropic fibre in the entire measuring optical scheme, which considerably simplifies the manufacturing of an optical coherence tomograph itself and interchangeable probes. The method can be used not only to obtain information successively upon scanning by varying the difference of the interferometer arms but also to obtain information rapidly (in parallel) by using tunable lasers. This variant of CP OCT method can be used to study the depolarising properties of biological tissues and determine birefringence parameters.

The portable device based on an isotropic fibre developed in our work is intended for CP OCT applications in clinics.

Acknowledgements. This work was partially supported by Russian State Contract 02.522.11.2002, 27 April 2007 and the Russian Foundation for Basic Research (Grant Nos 07-02-01090 and 07-08-00803).

References

1. Huang D., Swanson E.A., Lin C.P., Schuman J.S., Stinson W.G., Chang W., Hee M.R., Flotte T., Gregory K., Puliafito C.A., Fujimoto J.G. *Science*, **254**, 1178 (1991).
2. Sergeev A.M., Gelikonov V.M., Gelikonov G.V., Feldchtein F.I., Kuranov R.V., Gladkova N.D., Shakhova N.M., Snopova L.B., Shakhov A.V., Kuznetzova I.A., Denisenko A.N., Pochinko V.V., Chumakov Y.P., Streltzova O.S. *Opt. Express*, **1**, 432 (1997).
3. Hee M.R., Huang D., Swanson E.A., Fujimoto J.G. *J. Opt. Soc. Am.*, **9**, 903 (1992).
4. De Boer J.F., Milner T.E., van Gemert M.J.C., Nelson J.S. *Opt. Lett.*, **22**, 934 (1997).
5. Everett M.J., Schoenenberger K., Colston B.W. Jr., Da Silva L.B. *Opt. Lett.*, **23**, 228 (1998).
6. Schmitt J.M., Xiang S.H. *Opt. Lett.*, **23**, 1060 (1998).
7. De Boer J.F., Srinivas S.M., Malekafzali A., Chen Z.P., Nelson J.S. *Opt. Express*, **3**, 212 (1998).
8. Feldchtein F.I., Gelikonov G.V., Gelikonov V.M., Iksanov R.R., Kuranov R.V., Sergeev A.M., Gladkova N.D., Ourutina M.N., Warren J.A. Jr., Reitze D.H. *Opt. Express*, **3**, 239 (1998).

9. De Boer J.F., Milner T.E., Nelson J.S. *Opt. Lett.*, **24**, 300 (1999).
10. De Boer J.F., Srinivas S.M., Park B.H., Pham T.H., Chen Z.P., Milner T.E., Nelson J.S. *IEEE J. Sel. Top. Quantum Electron.*, **5**, 1200 (1999).
11. Saxer C.E., de Boer J.F., Park B.H., Zhao Y.H., Chen Z.P., Nelson J.S. *Opt. Lett.*, **25**, 1355 (2000).
12. Roth J.E., Kozak J.A., Yazdanfar S., Rollins A.M., Izatt J.A. *Opt. Lett.*, **26**, 1069 (2001).
13. Sankaran V., Walsh J.T., Maitland D.J. *J. Biomed. Opt.*, **7**, 300 (2002).
14. Stockford I.M., Morgan S.P., Chang P.C.Y., Walker J.G. *J. Biomed. Opt.*, **7**, 313 (2002).
15. De Boer J.F., Milner T.E. *J. Biomed. Opt.*, **7**, 359 (2002).
16. Pierce M.C., Park B.H., Cense B., de Boer J.F. *Opt. Lett.*, **27**, 1534 (2002).
17. Cense B., Chen T.C., Park B.H., Pierce M.C., de Boer J.F. *Opt. Lett.*, **27**, 1610 (2002).
18. Jiao S.L., Yu W.R., Stoica G., Wang L.H.V. *Opt. Lett.*, **28**, 1206 (2003).
19. Choma M.A., Sarunic M.V., Yang C., Izatt J.A. *Opt. Express*, **11**, 2183 (2003).
20. Dave D.P., Akkin T., Milner T.E. *Opt. Lett.*, **28**, 1775 (2003).
21. Cense B., Chen H.C., Park B.H., Pierce M.C., de Boer J.F. *J. Biomed. Opt.*, **9**, 121 (2004).
22. Guo S.G., Zhang J., Wang L., Nelson J.S., Chen Z.P. *Opt. Lett.*, **29**, 2025 (2004).
23. Chen Y., Otis L., Piao D., Zhu Q. *Appl. Opt.*, **44**, 2041 (2005).
24. Jiao S., Todorovic′ M., Stoica G., Wang L.V. *Appl. Opt.*, **44**, 5463 (2005).
25. Fan C., Wang Y., Wang R.K. *Opt. Express*, **15**, 7950 (2007).
26. Chen Z., Milner T.E., Dave D., Nelson J.S. *Opt. Lett.*, **22**, 64 (1997).
27. Kuranov R.V., Sapozhnikova V.V., Shakhova N.M., Gelikonov V.M., Zagainova E.V., Petrova S.A. *Kvantovaya Elektron.*, **32**, 993 (2002) [*Quantum Electron.*, **32**, 993 (2002)].
28. Kuranov R.V., Sapozhnikova V.V., Turchin I.V., Zagainova E.V., Gelikonov V.M., Kamensky V.A., Snopova L.B., Prodanetz N.N. *Opt. Express*, **10**, 707 (2002).
29. Fried D., Xie J., Shafi S., Featherstone J.D., Breunig T.M., Le C. *J. Biomed. Opt.*, **7**, 618 (2002).
30. Gelikonov V.M., Gelikonov G.V., Gladkova N.D., Kuranov R.V., Nikulin N.K., Petrova G.A., Pochinko V.V., Pravdenko K.I., Sergeev A.M., Feldshtein F.I., Khanin Ya.I., Shabanov D.V. *Pis'ma Zh. Eksp. Teor. Fiz.*, **61**, 149 (1995) [*JETP Lett.*, **61**, 158 (1995)].
31. Lefevre Y.C. *Electron. Lett.*, **16**, 778 (1980).
32. Feldchtein F.I., Gelikonov V.M., Gelikonov G.V., Gladkova N.D., Leonov V.I., Sergeev A.M., Khanin Y.I. *Optical Fiber Interferometer and Piezoelectric Modulator*. Patent US 5835642, 1998.
33. Feldchtein F., Bush J., Gelikonov G., Gelikonov V., Piyevsky S. *Proc. SPIE Int. Soc. Opt. Eng.*, **5690**, 349 (2005).
34. Gelikonov V.M., Gelikonov G.V. *Laser Phys. Lett.*, **3**, 445 (2006).
35. Alekseev E.I., Bazarov E.N., Izraelyan V.G. *Kvantovaya Elektron.*, **11**, 397 (1984) [*Sov. J. Quantum Electron.*, **14**, 271 (1984)].
36. Korn G.A., Korn T.M. *Mathematical Handbook for Scientists and Engineers* (New York: McGraw-Hill, 1961; Moscow: Nauka, 1971).
37. Bush J., Devis P.G., Marcus M.A. *Proc SPIE Int. Soc. Opt. Eng.*, **4204**, 71 (2001).
38. Drake A.D., Leiner D.C. *Rev. Sci. Instrum.*, **55**, 162 (1984).
39. Bush J., Feldchtein F.I., Gelikonov G.V., Gelikonov V.M., Piyevsky S. *Proc. SPIE Int. Soc. Opt. Eng.,* **5855**, 254 (2005).
40. Sharma U., Fried N.M., Kang J.U. *IEEE J. Sel. Top. Quantum Electron.*, **11**, 799 (2005).
41. Gelikonov V.M., Leonov V.I., Novikov M.A. *Volokonno-opticheskii datchik* (Fibreoptic Sensor), USSR Inventor's Certificate No. 1315797 A1. *Byull. Izobret.*, No. 24, 3 (1987).
42. Gelikonov V.M., Gusovskii D.D., Leonov V.I., Novikov M.A. *Pis'ma Zh. Tekh. Fiz.*, **13**, 775 (1987) [*Sov. Tech. Phys. Lett.*, **13**, 322 (1988)].
43. Olsson N.A. *Electron. Lett.*, **24**, 1075 (1988).
44. Martinelli M. *Opt. Commun.*, **72**, 341 (1989).
45. Pistoni N.C., Martinelli M. *Proc. 7th Optical Fiber Sensors Conf.* (Sydney, Australia: IEEE, 1990) p. 125.
46. Pistoni N.C., Martinelli M. *Opt. Lett.*, **16**, 711 (1991).
47. Van Deventor M.D. *Electron. Lett.*, **27**, 1538 (1991).
48. Sorin W.V., Baney D.M. *IEEE Photonic. Technol. Lett.*, **4**, 1404 (1992).